Lagrangian simulation of mixing and reactions in complex geochemical systems

Nicholas B. Engdahl[1], David A. Benson[2], and Diogo Bolster[3]

[1]Civil and Environmental Engineering, Washington State University

[2]Hydrologic Science and Engineering, Colorado School of Mines

[3]Civil and Environmental Engineering and Earth Sciences, University of Norte Dame

This article has been accepted for publication and undergone full peer review but has not been through the copyediting, typesetting, pagination and proofreading process which may lead to differences between this version and the Version of Record. Please cite this article as an 'Accepted Article', doi: 10.1002/2017WR020362

Abstract. Simulations of detailed geochemical systems have traditionally been restricted to Eulerian reactive transport algorithms. This note introduces a Lagrangian method for modeling multi-component reaction systems. The approach uses standard random walk based methods for the particle motion steps but allows the particles to interact with each other by exchanging mass of their various chemical species. The colocation density of each particle pair is used to calculate the mass transfer rate, which creates a local disequilibrium that is then relaxed back toward equilibrium using the reaction engine PhreeqcRM. The mass exchange is the only step where the particles interact and the remaining transport and reaction steps are entirely independent for each particle. Several validation examples are presented, which reproduce well-known analytical solutions. These are followed by two demonstration examples of a competitive decay chain and an acid-mine drainage system. The source code, entitled Complex Reaction on Particles (CRP), and files needed to run these examples are hosted openly on GitHub (https://github.com/nbengdahl/CRP), so as to enable interested readers to readily apply this approach with minimal modifications.

1. Introduction

Direct simulations of complex geochemical systems have remained challenging for many decades because they involve tightly coupled transport and reaction processes. The typical approach for these kinds of models in the past has been to simplify one aspect of the problem so that more attention can be paid to the other. This has generally split research on the topic into studies that focus on detailed geochemistry while simplifying mixing processes [e.g. *Mayer et al.*, 2006; *Pedretti et al.*, 2015; *Gardner et al.*, 2015], and those that make the opposite tradeoff for the purpose of upscaling [e.g. *Donado et al.*, 2009; *Le Borgne et al.*, 2015]. The studies focusing on geochemistry have led to the development of advanced geochemical tools like PFLOTRAN [*Mills et al.*, 2007; *Scheibe et al.*, 2015; *Hammond et al.*, 2014], CrunchFlow [*Steefel and Lasaga*, 1994; *Steefel et al.*, 2015; *Beisman et al.*, 2015], and PHREEQC [*Prommer et al.*, 2003; *Appelo and Rolle*, 2010], among others. These tools allow simulations of complex geochemistry with transport for a wide range of environmentally relevant chemical processes, but all are Eulerian (grid-based) methods. Consequently they all assume complete mixing at the scale of the cell size of the model, which is also the support scale assumed for the mean velocity. This is not to say that Eulerian methods cannot be used to study mixing limited reactive transport, but the resolution of the model dictates the level of chemical variability that can be accurately simulated. Without an upscaled model to bridge the scales, Eulerian simulations require high-resolution grids to resolve fine-scale heterogeneity, which can impart immense computational costs. These methods can also suffer from numerical dispersion, and associated spurious mixing, when simulating the advective portion of the transport, which can lead

to incorrect estimates of the extents of solute plumes and overall rates of reaction [*Cui et al.*, 2014; *Benson et al.*, 2017].

The role of mixing on reaction rates has also seen much attention recently, but these advances have focused on very fundamental aspects and thus revolved around elementary, bi-molecular reactions [*Raje and Kapoor*, 2000; *Gramling et al.*, 2002; *Le Borgne et al.*, 2010; *Paster et al.*, 2015]. These studies have led to great leaps in our understanding of mixing processes and their impact on reactions, but many of the assumptions required by the mathematical models can be limiting to the point that the approach or results of one study cannot easily be generalized to other reaction systems or initial conditions. However, in contrast to the geochemical studies, much of the work on mixing has used Lagrangian methods to simulate transport, which have traditionally been used for conservative transport or first order decay [e.g. *LaBolle et al.*, 1996; *Salamon et al.*, 2006]. However, there are now an ever growing number of examples where reactions between random walk particles can be simulated [e.g. *Ma et al.*, 1999; *Benson and Meerschaert*, 2008; *Ding et al.*, 2013; *Bolster et al.*, 2016]. To date though, these have relied on elementary reactions that are hard-wired into the solvers and have not been generalized to mixtures with complex geochemistry, such as multi-component transport, electrical or pH effects, speciation/complexation, and multi-step, competitive reactions. To date, Eulerian methods have a clear advantage for simulating reactive transport in this regard because, to our knowledge, few robust particle-based equivalents exist.

This note introduces a Lagrangian reactive transport tool that allows simulations of complex reactions on particles, abbreviated hereafter as "CRP." The new algorithm generalizes recent developments in particle tracking methods beyond the simple elementary

reactions that have been prevalent in the mixing and reaction literature to date. The new method allows complex multi-step reactions, nonlinear reactions, and any combination of equilibrium and kinetic reactions involving any number of chemical components. The method simulates advection and hydrodynamic dispersion through "parent" particles that transport arbitrarily complex mixtures through the domain. After a transport step, the different parent particles exchange masses of their individual components. The composition of each parent particle is then relaxed toward its local chemical equilibrium in a reaction step where the masses of the components are adjusted using the PhreeqcRM reaction module [*Parkhurst and Wissmeier*, 2015]. The motivation for this note is to present a new method that combines a number of recent advances; a second aim is to make available a fully operational code. To this end, we have provided the code and all files needed to generate the results we present here on GitHub (https://github.com/nbengdahl/CRP), all of which can be run in Matlab. Users will first need to install the PhreeqcRM library but this is the only additional step needed to reproduce the examples, which are otherwise self-contained.

2. Simulating complex reactions on particles

2.1. Particle colocation and mass exchange

The basic elements of random walk particle tracking methods can be found in work by *LaBolle et al.* [1996] and *Salamon et al.* [2006]. Here we use only dimensionless quantities (*i.e.* time, concentration, distance, etc...) but this is not a requirement. The original method for simulating bimolecular reactions on particles is described by *Benson and Meerschaert* [2008], *Ding et al.* [2013] and *Paster et al.* [2013]. It calculate the probability of reaction by combining the probability that two particles will be colocated and the

thermodynamic probability that two particles will react, given colocation: $P(\text{react}) = P(\text{react}|\text{colocation}) \times P(\text{colocation})$. The latter colocation probability depends on time interval and separation:

$$P(\mathbf{s}|\Delta t) = \int_{\Delta s} \nu(\mathbf{s}|\Delta t) d\mathbf{s} \approx \nu(\mathbf{s}|\Delta t)\Delta\mathbf{s} \tag{1}$$

where $\nu()$ is the colocation density function, $\mathbf{s}$ is the distance between two particles, Δt is the time step and $\Delta\mathbf{s}$ is a length/area/volume represented by a particle in d-dimensions. When this is small, the first-order approximation is appropriate. Because a particle has finite support, there is a local-scale dispersion tensor associated with every particle's random motion. At the smallest scale this may be primarily due to molecular diffusion, but for general Fickian dispersion the colocation density function is:

$$\nu_{i,j}(\mathbf{s}|\Delta t) = \frac{\exp\left[-\frac{1}{4\Delta t}\mathbf{s}^T(\mathbf{D}_i + \mathbf{D}_j)^{-1}\mathbf{s}\right]}{\sqrt{(4\pi\Delta t)^d \det[\mathbf{D}_i + \mathbf{D}_j]}} \tag{2}$$

where $\mathbf{D}$ are n-dimensional dispersion tensors associated with each particle, and i and j are indices over particle pairs. This equation arises from the convolution of two Gaussian density functions, which are the particle position density functions [*Engdahl et al.*, 2014]. The original simulation approach, for bi-molecular reactions, was to visit every pair of particles with different chemical species in a randomized order, evaluate the probability of colocation of each neighbor relative to a uniform random number, and either react or take a diffusive step accordingly. Reactions between two particles were implemented with a particle killing algorithm: if two particles were found to react, then both were removed from the simulation. More complex reactions required a sequence of mono- or bi-molecular reactions [*Ding and Benson*, 2015]. The algorithm was recently modified to preserve the particle number by *Bolster et al.* [2016], allowing each particle to have its

mass reduced by interactions with other particles instead of killing entire particles. In each case, advective, diffusive, and dispersive motion, or other less traditional transport mechanisms [e.g. *Bolster et al.*, 2012], could also be included but the main limitation with all these approaches is that only single-step mono- or bi-molecular reactions could be simulated.

Benson and Bolster [2016], building on *Bolster et al.* [2016], recently derived a new approach where particles carry any number of chemical species. After advective and dispersive motion, the particles exchange mass of all species, then engage in a kinetic reaction that is evaluated on each particle. The novel step of this process is the algorithm that exchanges mass between the different "parent" particles, which recognizes that the colocation density can also be interpreted as a weight function describing mass transfer quantities based on separation distance. All particles that are close enough to colocate exchange some mass proportional to $\nu_{i,j}(\mathbf{s})$, and this leads to a simple expression for the mass transfer between all particles in the ensemble. For the mass m of each chemical species on the j^{th} particle:

$$m_j(t+\Delta t) - m_j(t) = \frac{1}{2}\sum_{i\neq j}(m_i - m_j)^* \nu_{i,j}(\mathbf{s}|\Delta t)\Delta\mathbf{s} \tag{3}$$

where * denotes the time at which masses are used in the calculation: masses may updated while looping through the particles in a semi-explicit sense [*Benson and Bolster*, 2016], or * may denote masses at the $t+\Delta t$ timestep in which an implicit calculation is conducted by

$$\left(1+\frac{1}{2}\sum_{i\neq j}\nu_{i,j}(\mathbf{s}|\Delta t)\Delta\mathbf{s}\right)m_j(t+\Delta t)-$$
$$\frac{1}{2}\sum_{i\neq j}\nu_{i,j}(\mathbf{s}|\Delta t)\Delta\mathbf{s})m_i(t+\Delta t)=m_j(t) \quad (4)$$

This can be written in matrix notation $V \times m(t+\Delta t) = m(t)$, where m is a vector of particle masses and V is size $n_P \times n_P$, where the main diagonal is the first term in parentheses in (4) and entries off the main diagonal contain the terms $v_{i,j}(\mathbf{s})\Delta\mathbf{s}$. In practice, many of the colocation densities are negligible and fast search algorithms can be used to efficiently build a sparse matrix, but the full matrix is shown here because it is simple to implement.

The key point is that (3), or a similar implementation, allows the particles to interact and exchange mass for any number of chemical components, and each may use a different dispersion tensor for each. Lack of interaction has been the main limitation for implementing complex reactions in a particle tracking framework to date.

2.2. Reaction engine

Conceptually, mass exchange mixes the composition of solutes associated with each particle, which is then relaxed back toward the local chemical equilibrium by evaluating specific reaction mechanisms. The new CRP model presented here adopts the recently developed PhreeqcRM component library [*Parkhurst and Wissmeier*, 2015] as the reaction engine. Details for using the library are given by *Parkhurst and Wissmeier* [2015] with additional, relevant, notes in *Charlton and Parkhurst* [2011]. PhreeqcRM contains the reaction modules behind the popular geochemical code PHREEQC in a package specifically designed for operator-splitting based simulations of reactive transport. The source code

is freely available (*wwwbrr.cr.usgs.gov/projects/GWC_coupled/phreeqc/*) and our model uses version 3.3.8 build 11728 of the library accessed in late October of 2016. The mass exchange and motion steps of the transport algorithm are coded in Matlab and the PhreeqcRM modules are called as needed. We also note that the PhreeqcRM package is easily configured for multi-threading applications, providing reasonable speedup of simulations.

The basic workflow is to define the number of particles and their initial positions, load a geochemical database, assign solution chemistries and reaction properties, define physical and thermodynamic properties (saturation, porosity, temperature, pH, etc...), and then define the initial condition. PhreeqcRM calculates reactions based on species within a "cell," which is independent of all others, so we pass the species on a particle to a PhreeqcRM cell. Different kinetic reactions can be defined in different cells, and different equilibrium phases (minerals) can also be included, amongst many other options; we refer the reader to the PhreeqcRM documentation for more detail. The transport step is evaluated next, which may be a combination of advection, diffusion, and mechanical dispersion, followed by a mass exchange step (Eq. 3), then the PhreeqcRM model is called to simulate the relaxation of the solution in each cell, and the process repeats. An important point is that, in principle, this approach is no different than the way that one would evaluate geochemical interactions in an operator-splitting manner for an Eulerian model, but here the Lagrangian elementary volume is considered to be the region around the particle instead of a fixed grid cell.

3. Model validation

The purpose of this section is to demonstrate that the new approach is able to reproduce reaction mechanisms in the common "benchmark" examples. This includes equilibrium

and kinetic reactions that are reversible and irreversible. Since these are all well-studied reaction systems, we provide only a minimal discussion, focusing on any departures from known solutions.

3.1. Irreversible kinetic reaction

The first comparison we make is to the bimolecular kinetic reaction:

$$A + B \underset{k_r}{\overset{k_f}{\rightleftharpoons}} C \tag{5}$$

where k_f and k_r are the forward and backward reaction rate constants and a unit activity coefficient is assumed for simplicity. The rate laws for this reaction are assumed to be:

$$\frac{d[A]}{dt} = \frac{d[B]}{dt} = -k_f[A][B] + k_r[C] \tag{6a}$$

$$\frac{d[C]}{dt} = k_f[A][B] - k_r[C] \tag{6b}$$

where [ ] denotes concentration. If the initial concentration of A and B are equal and $k_r = 0$, an analytic solution is easy to solve:

$$[A]/[A]_0 = [1 + k_f[A]_0 t]^{-1} \tag{7}$$

The irreversible kinetic reaction, Eq. (6) with $k_r = 0$, was defined within PhreeqcRM and simulated in 1-d from the initial condition up to 100 time units with a time step of $\Delta t = 0.1$, $k_f = 1$ and $D = 1.0\text{x}10^{-2}$ in a domain of total length $L = 1$ centered at the origin with zero flux boundary conditions in a diffusion-only scenario. The initial masses of A and B were distributed randomly among 1,000 particle positions spread evenly along the x-axis to simulate a well-mixed system and no C is initially present. Initially, half of the particles are given 100% A and the other half 100% B at concentrations of 2. This provides an initial domain-wide average concentration of unity but also requires mass

transfer for the reaction to proceed. These parameters give a particle Damkohler number [see *Benson and Bolster*, 2016] of $Da = k_f[A]_0(L/N)^2/D = 10^{-4}$, indicating a well-mixed system. The characteristic diffusion length is given by the average inter-particle spacing. Particle positions are held constant in this simulation so that all diffusion is simulated via mass-exchange. The average product concentration in the domain over time is shown in Figure 1 for the CRP simulation ("Well-mixed") along with the analytical solution ("Analytical"), which are in excellent agreement. A slight variation on the problem is one where the distribution of the initial masses are split into each half, which is a classic mixing interface problem. The only modification is that A is placed exclusively within $x < 0$ and only B is placed within $x > 0$. Now the Damkohler number is approximately $Da = k_f[A]_0(L/2)^2/D = 25$, indicating a moderately poorly-mixed system. The simulation was re-run over the same time interval and the effect of the mixing limitation is immediately apparent (Figure 1, "Limited"). The two solutions must now mix before the reaction can start. The effect is an initial decrease in the reaction rate that much later approaches the well-mixed rate, typical of mixing-limited systems in finite domains [*Bolster et al.*, 2011; *Le Borgne et al.*, 2011]. The late-time behavior converges to the well-mixed rate, reflecting the time for homogenization.

The lack of an analytical solution for the mixing-limited case makes it difficult to determine whether or not the simulation is accurate. The particle based solution was compared to an equivalent implicit finite-difference solution of the diffusion equation, that also used PhreeqcRM as the reaction engine (note that an identical finite-difference result is obtained using the diffusion model within the standard PHREEQC model). The domain was discretized onto 200 evenly spaced cells and the same sharp initial condition was im-

posed on the system. The concentration from the finite difference model for the product is shown as the dashed line in Figure 1 and the methods show good agreement, providing a cross-validation.

3.2. Equilibrium reaction

Another variation on this problem with a simple analytical solution is the case where the kinetic reaction of (6) is exchanged for an equilibrium reaction, while keeping the same chemical equation. In this case, $d[A]/dt = d[C]/dt = 0$ and a solution to (6) is $[C]/[A][B] = k_f/k_r \equiv K_{eq}$. This example will use the mixing-limited initial condition where half of the problem domain will be initially filled with A and the other with B, and the reaction is irreversible, so $k_r = K_{eq} = 0$ (or equivalently, the forward reaction is instantaneous, so $k_f = \infty$). This is the well-known irreversible reaction from *Gramling et al.* [2002], who include an analytical solution.

The simulation parameters and model configuration were translated into PhreeqcRM and simulated with the new CRP model. Particles ($n_P = 1000$) were randomly placed in the same domain as the previous example and the same diffusion coefficient as above is used, but we allow diffusion by random walks and mass transfer (by Eq. 3) to occur. The time series of product and reactant masses are shown in Figure 2 along with a comparison to the analytical solution. The blue lines and dots are the irreversible reaction and a reversible equilibrium reaction is shown in red for comparison that favors the reactants ($\log K_{eq} = -1.0$). The analytical solution is for an infinite domain so any numerical simulation will depart from it but it is clear that prior to encountering the boundary effects the scaling of the simulation and analytical solution are identical. The reversible

case differs in that the reactants are not entirely consumed and that the amount of product mass is lower as a consequence.

The departure from the analytical solution makes it difficult to determine whether or not the correct late behavior is reached so the reversible and irreversible equilibrium reaction problems were also simulated using an implicit finite-difference solution. The concentration curves from the finite-difference model are shown as the dashed black lines in Figure 2. The particle simulations exhibit a small departure from the analytical solutions at early times. This is a consequence of the mass transfer model since Eq. 3 requires a few time steps for particles to migrate into "contact" with each other when diffusion is simulated via mass transfer. Despite this, the reversible and irreversible reactions both compare well for the different solution methods.

3.3. Reversible kinetic reaction

Lastly, we consider the case where the previous kinetic reaction is made reversible. The solution to the well-mixed case is found by numerical integration of Eq. (6) using the "ode45" function in Matlab. The forward rate constant is increased from the last example $k_f = 2.0\text{x}10^{-1}$ and the reverse rate constant is $k_r = 1.5\text{x}10^{-2}$ to place the reaction on the same time scale as the previous example. The simulation also uses a smaller number of particles, $n_P = 750$, a constant time step of $\Delta t = 0.1$, and the initial concentrations of A and B in the domain are equal. The particle and ODE solver based results for these parameters and a second set of parameters ($k_f = 1.0\text{x}10^{-2}$ and $k_r = 1.0\text{x}10^{-3}$) are shown in Figure 3. We also numerically verified that $K_{eq} = k_f/k_r$ was suitably close to $([C]_{eq}/[A]_{eq}[B]_{eq})$, where $[x]_{eq}$ denotes the calculated species concentrations at equilibrium.

4. Complex reaction systems

So far all of our examples have been simple and were shown to validate the coupling with PhreeqcRM in a context where solutions are readily available. They have shown that the model is accurate for the four most basic reaction types. This section uses more complex reactions that are solvable using the PhreeqcRM engine.

4.1. Degradation chain

The first example is loosely based on the decay-chain concept from the PHAST model [*Parkhurst et al.*, 2004] but with heterogeneous reaction mechanisms. The hypothetical system involves a reaction chain where the following generic reactions can occur:

$$A + B \rightarrow C \tag{8a}$$

$$C + E \leftrightharpoons CE \tag{8b}$$

$$E \rightarrow \varnothing \tag{8c}$$

Equation (8a) is an irreversible kinetic reaction with rate $k_f = 1.0$, (8b) is a reversible equilibrium reaction with $\log_{10}(k_{eq}) = 5$, and E undergoes first order decay at a rate $\lambda_E = 1.0\text{x}10^{-1}$ (8c). Depending on how each component is defined, and some changes to the stoichiometry and rate constants, this could represent any number of reaction systems such as aerobic degradation or nitrate reduction.

We define a 1-D domain, $L = 10$, with periodic boundaries and $n_P = 2000$ randomly placed particles that exchange mass and also experience diffusion. The initial conditions for A and B are split so that A resides in $x < 5$ and B is exclusively in $x > 5$, with concentrations of 1.0 and 1.15, respectively. The initial concentration of E is 1.25, residing only in $x < 5$. The remaining products, CE and C, begin with no mass. The decay

reaction of E is also restricted to only 20% of the domain, selected randomly, which is meant to represent a heterogeneous distribution of minerals, microorganisms, catalysts, or any number of other factors (physical or chemical) that effect the reactions' progress.

The system was simulated for 1000 time units at a constant time step $\Delta t = 0.1$ and the results for the average concentration in the domain over time are shown in Figure 4. At early times, the reaction system is limited by the mixing of A and B because C must be produced before the second reaction (Eq. 8b) can start. The rapid production of C allows faster formation of CE, which sequesters some of the E. However, at late time the remaining mass of E is depleted and the reverse reaction of (8b) begins to dominate. Since this system has no analytical solution, we again compare the result to an implicit-in-time finite-difference solution of the diffusion equation for each species discretized on 200 evenly spaced cells. These resulting concentration curves are shown as the dashed black lines and the two methods are in good agreement.

4.2. Acid mine drainage

We finish with a much more complex and practically relevant example. Acid-mine drainage (AMD) is a problem in many parts of the world that leads to the formation and mobilization of metals and nanoparticles among other aqueous contaminants. At many sites, metal-sulfide minerals in tailings from mining operations are left exposed near the land surface, and a combination of rainfall and an oxygen-rich environment mobilize various contaminants. A full simulation of watershed dynamics and transport for a specific site is beyond the scope of this note, but some key elements can be demonstrated in a still complex, but simpler system. Natural systems tend towards an equilibrium and the same is true of AMD systems, so understanding how the system will respond to perturbations

is often important. Many AMD sites are in mountainous terrain that are seasonally influenced by snowmelt, so we will consider how a relatively stable AMD flow system responds to a pulse of clean snowmelt. The geochemistry of this problem is based on *Mayer et al.* [2006] and *Pedretti et al.* [2015] and interested readers are referred there for more details on AMD problems.

The conceptual model for this example is a river flowing over outcrops of iron rich deposits or through piles of mine tailings. The domain is centered at the origin with a total length $L = 10$ where the region $-1.5 < x < 1.5$ is in equilibrium with pyrite (saturation index of 1); the remaining regions have no reactive mineral phases and function as mixing zones. The simulation uses 2000 particles and 500 of these are held at fixed positions (immobile) to represent the pyrite rich outcrop. This restricts the reactions with the equilibrium mineral phase to only 30% of the domain but competitive aqueous equilibration reactions will happen throughout the system as a result of mixing. Periodic boundaries are defined so that the model represents the sequential change in chemistry as the water moves over several outcrops. The geochemistry of the initial condition is modified after *Mayer et al.* [2006] but we omit calcium to reduce the number of species and deplete the system in carbon to reduce its buffering effect.

The composition of the initial condition is based on initial SO_4^{-2}, Fe^{+2}, and CO_3^{-2} molal concentrations of $2.2\text{x}10^{-2}$, $3.2\text{x}10^{-2}$, and $8.3\text{x}10^{-8}$, respectively, which are given one time step to equilibrate with pyrite before the reactive transport simulation beings. The clean water is added as a block of 500 particles, located 1.5 units upstream from the outcrop. Reactions were simulated using the "phreeqc.dat" database file and we allow a 50/50 mixture of mass transfer and random walk diffusion to simulate mixing, a constant

velocity of $v = 0.5$ [LT^{-1}], and a dispersivity coefficient of $\alpha_L = 0.1$ [L]. The simulation was run forward for 150 time units at a time step of $\Delta t = 0.1$ and the resulting total masses for selected aqueous species over time are shown in Figure 5.

The Fe^{+3} and sulfate species respond most rapidly to the perturbation and the periodic movement of the clean water slug past the outcrop can be seen in the H_2S signal. This system only involves equilibrium reactions so any variation in reaction rates is due to mixing, which can have complicated effects on the solution over time. The spatial distribution of selected aqueous species at $t = 15$ is shown in Figure 6, where some of the concentrations have been scaled to facilitate comparisons (scale factors are given in parentheses).

5. Discussion

The point of the examples presented in section 4 is not to study the detailed geochemical processes but rather to demonstrate the complex reactions that can be included in a particle based simulation. The novelty of the AMD example of section 4.2 is that it allows geochemical interactions between static and mobile particles. A number of improvements could be made to the algorithm, including adaptive time stepping, more efficient search algorithms for the mass exchange step, and the use of kernels to reduce particle numbers (*Schmidt et al.* [2016 (in press]; *Rahbaralam et al.* [2015]). There are also several open questions regarding how one might interpolate the concentrations assigned to each particle on to an Eulerian grid (to compare to field monitoring data, for example) and the numerical effects (including operator splitting) on solution accuracy [e.g., *Paster et al.*, 2013].

The main advantages of particle methods are speed and accuracy, as highlighted in a recent article by *Benson et al.* [2017]. A runtime comparison was omitted here because the

gains are inconsequential for these 1-D examples, but we expect significant performance gains in 3-D simulations. Another advantage is that mixing and chemical heterogeneity are accurately resolved at the scale of the particles [see *Paster et al.*, 2014], not the mean velocity, unlike Eulerian or mixed Eulerian/Lagrangian methods that map particle masses to gridded concentrations [*Tompson and Dougherty* , 1992]. One application where the CRP approach is well-suited is tracing sharp pulses, such as the AMD example of section 4.2, where transport and reactions are restricted to a subset of a large domain. In this case, the number of geochemical calculations can be significantly reduced, from the number of grid cells in the domain to the number of particles. A key question regarding the CRP approach is when should it be used instead of an Eulerian method. There is no simple answer to this without a detailed study of both approaches under a variety of conditions, including 1-, 2-, and 3-dimensional systems, with different amounts of physical and chemical heterogeneity. As with all methods there will clearly be situations where Eulerian approaches may be advantageous and others where Lagrangian ones are best. For a discussion highlighting such cases for conservative transport see *Boso et al.* [2013].

This note has shown that complex reactions on particles can be simulated by combining particle-based methods of transport with a mass-exchange algorithm and the general PhreeqcRM reaction engine. The result is a flexible reactive transport platform that is able to reproduce all of the common elementary reactions used for model validation, which are common in studies on mixing-limited reactive transport. The key difference between this approach and previous Lagrangian reaction simulations is that the reaction can involve any number of species and any number of reactions, either from the PHREEQC database or any user defined reactions. The code needed to reproduce these examples is provided

on GitHub (https://github.com/nbengdahl/CRP), but users will need to first install the PhreeqcRM library in order to run them.

Acknowledgments. The authors thank Reza Soltanian, Matthias Willmann, and an anonymous reviewer for helpful and constructive feedback that improved the manuscript. This work was supported by the National Science Foundation [grant numbers EAR-1417145, EAR-1351625, and EAR-1417264]. The figures presented here can be generated directly from the information provided but the provided link (https://github.com/nbengdahl/CRP) includes example run files that reproduce the results. The data can also be obtained from the corresponding author.

References

Appelo, C. A. J., and M. Rolle (2010), PHT3D: A reactive multicomponent transport model for saturated porous media, *Ground Water*, *48*(5), 627–632, doi:10.1111/j.1745-6584.2010.00732.x.

Bear, J. (1972), *Dynamics of Fluids in Porous Media*, Dover Books reprint of American Elsevier Publishing Company, Inc., New York.

Beisman, J. J., R. M. Maxwell, A. K. Navarre-Sitchler, C. I. Steefel, and S. Molins (2015), ParCrunchFlow: an efficient, parallel reactive transport simulation tool for physically and chemically heterogeneous saturated subsurface environments, *Computational Geosciences*, *19*, 403–422, doi:10.1007/s10596-015-9475-x.

Benson, D. A., and D. Bolster (2016), Arbitrarily complex chemical reactions on particles, *Water Resources Research*, *52*, doi:10.1002/2016WR019368.

Benson, D. A., and M. M. Meerschaert (2008), Simulation of chemical reaction via particle tracking: Diffusion-limited versus thermodynamic rate-limited regimes, *Water Resources Research*, *44*(12), 1–7, doi:10.1029/2008WR007111.

Benson, D. A., T. Aquino, D. Bolster, N. Engdahl, C. V. Henri, and D. Fernàndez-Garcia (2017), A comparison of Eulerian and Lagrangian transport and non-linear reaction algorithms, *Advances in Water Resources*, *99*, 15 – 37, doi: http://dx.doi.org/10.1016/j.advwatres.2016.11.003.

Bolster, D., M. Dentz, and T. Le Borgne (2011), Hypermixing in linear shear flow, *Water Resources Research*, *47*(9), 1–5, doi:10.1029/2011WR010737.

Bolster, D, P de Anna, DA. Benson, and AM. Tartakovsky. Incomplete mixing and reactions with fractional dispersion. Advances in Water Resources 37 (2012): 86-93.

Bolster, D., A. Paster, and D. A. Benson (2016), A particle number conserving Lagrangian method for mixing-driven reactive transport, *Water Resources Research*, *52*, 1518—1527, doi:10.1002/2015WR018310.

Boso, Francesca, Alberto Bellin, and Michael Dumbser (2013). Numerical simulations of solute transport in highly heterogeneous formations: A comparison of alternative numerical schemes. Advances in Water Resources 52 (2013): 178-189.

Charlton, S. R., and D. L. Parkhurst (2011), Modules based on the geochemical model PHREEQC for use in scripting and programming languages, *Computers and Geosciences*, *37*(10), 1653–1663, doi:10.1016/j.cageo.2011.02.005.

Cui, Z., Welty, C., and R. M. Maxwell (2014), Modeling nitrogen transport and transformation in aquifers using a particle-tracking approach, *Computers and Geosciences*, *70*, 1–4, doi:10.1016/j.cageo.2014.05.005.

Ding, D., and D. A. Benson (2015), Simulating biodegradation under mixing-limited conditions using michaelis–menten (monod) kinetic expressions in a particle tracking model, *Advances in Water Resources*, *76*, 109 – 119, doi: http://dx.doi.org/10.1016/j.advwatres.2014.12.007.

Ding, D., D. A. Benson, A. Paster, and D. Bolster (2013), Modeling bimolecular reactions and transport in porous media via particle tracking, *Advances in Water Resources*, *53*, 56–65, doi:10.1016/j.advwatres.2012.11.001.

Donado, L. D., X. Sanchez-Vila, M. Dentz, J. Carrera, and D. Bolster (2009), Multicomponent reactive transport in multicontinuum media, *Water Resources Research*, *45*(11), 1–11, doi:10.1029/2008WR006823.

Engdahl, N. B., D. A. Benson, and D. Bolster (2014), Predicting the enhancement of mixing-driven reactions in nonuniform flows using measures of flow topology, *Physical Review E*, *90*(5), 051001, doi:10.1103/PhysRevE.90.051001.

Gardner, W. P., G. Hammond, and P. Lichtner (2015), High Performance Simulation of Environmental Tracers in Heterogeneous Domains, *Ground Water*, *53*, 71–80, doi: 10.1111/gwat.12148.

Gramling, C. M., C. F. Harvey, and L. C. Meigs (2002), Reactive transport in porous media: a comparison of model prediction with laboratory visualization., *Environmental science & technology*, *36*(11), 2508–14.

Hammond, G. E., P. C. Lichtner, and R. T. Mills (2014), Evaluating the performance of parallel subsurface simulators: An illustrative example with PFLOTRAN, *Water Resources Research*, *50*(1), 208–228, doi:10.1002/2012WR013483.

LaBolle, E. M., G. E. Fogg, and A. F. B. Tompson (1996), Random-walk simulation of transport in heterogeneous porous media: Local mass-conservation problem and implementation methods, *Water Resources Research*, *32*(3), 583–593.

Le Borgne, T., M. Dentz, D. Bolster, J. Carrera, J.-R. de Dreuzy, and P. Davy, (2010), Non-Fickian mixing: Temporal evolution of the scalar dissipation rate in heterogeneous porous media, *Advances in Water Resources*, *33*(12),1468–1475.

Le Borgne, T., M. Dentz, P. Davy, D. Bolster, J. Carrera, J.-R. de Dreuzy, and O. Bour (2011), Persistence of incomplete mixing: A key to anomalous transport, *Physical Review E*, *84*(1), 1–4, doi:10.1103/PhysRevE.84.015301.

Le Borgne, T., M. Dentz, and E. Villermaux (2015), The lamellar description of mixing in porous media, *Journal of Fluid Mechanics*, *770*, 458–498, doi:10.1017/jfm.2015.117.

Ma, Y., M. W. Kemblowski, and G. E. Urroz (2006), A Heuristic Model of Aerobic Biodegradation of Dissolved Hydrocarbons in Aquifers, *Ground Water*, *37*(4), 491–497, doi:10.1111/j.1745-6584.1999.tb01134.x.

Mayer, K. U., S. G. Benner, and D. W. Blowes (2006), Process-based reactive transport modeling of a permeable reactive barrier for the treatment of mine drainage, *Journal of Contaminant Hydrology*, *85*(3-4), 195–211, doi:10.1016/j.jconhyd.2006.02.006.

Mills, R. T., C. Lu, P. C. Lichtner, and G. E. Hammond (2007), Simulating subsurface flow and transport on ultrascale computers using PFLOTRAN, *Journal of Physics: Conference Series*, *78*, 012,051, doi:10.1088/1742-6596/78/1/012051.

Parkhurst, D. L., and L. Wissmeier (2015), PhreeqcRM: A reaction module for transport simulators based on the geochemical model PHREEQC, *Advances in Water Resources*, *83*, 176–189, doi:10.1016/j.advwatres.2015.06.001.

Parkhurst, D. L., K. Kipp, P. Engesgaard, and S. R. Charlton (2004), PHAST - A program for simulating ground-water flow, solute transport, and multicomponent geochemical reactions, *USGS Techniques and Methods 6*, U.S. Geological Survey.

Paster, A., D. Bolster, and D. A. Benson (2013), Particle tracking and the diffusion-reaction equation, *Water Resources Research*, *49*(1), 1–6, doi:10.1029/2012WR012444.

Paster, A., D. Bolster, and D. A. Benson (2014), Connecting the dots: Semi-analytical and random walk numerical solutions of the diffusion–reaction equation with stochastic initial conditions, *Journal of Computational Physics*, *263*, 91–112.

Paster, A., T. Aquino, and D. Bolster (2015), Incomplete mixing and reactions in laminar shear flow, *Physical Review E*, *92*(1), 012,922, doi:10.1103/PhysRevE.92.012922.

Pedretti, D., A. Lassin, and R. D. Beckie (2015), Applied Geochemistry Analysis of the potential impact of capillarity on long-term geochemical processes in sulphidic waste-rock dumps, *Applied Geochemistry*, *62*, 75–83, doi:10.1016/j.apgeochem.2015.03.017.

Prommer, H., D. a. Barry, and C. Zheng (2003), MODFLOW/MT3DMS-based reactive multicomponent transport modeling, doi:10.1111/j.1745-6584.2003.tb02588.x.

Rahbaralam, M., D. Fernàndez-Garcia, and X. Sanchez-Vila (2015), Do we really need a large number of particles to simulate bimolecular reactive transport with random walk methods? A kernel density estimation approach, *Journal of Computational Physics*, *303*, 95–104, doi:10.1016/j.jcp.2015.09.030.

Raje, D. S., and V. Kapoor (2000), Experimental Study of Bimolecular Reaction Kinetics in Porous Media, *Environmental Science & Technology*, *34*(7), 1234–1239, doi:10.1021/es9908669.

Salamon, P., D. Fernandez-Garcia, and J. J. Gomez-Hernandez (2006), A review and numerical assessment of the random walk particle tracking method, *Journal of Contaminant Hydrology*, *87*(3-4), 277–305, doi:10.1016/j.jconhyd.2006.05.005.

Scheibe, T. D., X. Yang, X. Chen, and G. Hammond (2015), A Hybrid Multiscale Framework for Subsurface Flow and Transport Simulations, *Procedia Computer Science*, *51*, 1098–1107, doi:10.1016/j.procs.2015.05.276.

Schmidt, M., S. Pankavich, and D. A. Benson (2016 (in press)), A kernel-based Lagrangian method for imperfectly-mixed chemical reactions, *Journal of Computational Physics*, *http://dx.doi.org/10.1016/j.jcp.2017.02.012*.

Steefel, C., and A. Lasaga (1994), A Coupled Model for Transport of Multiple Chemical Species and Kinetic Precipitation/Dissolution Reactions with Application to Reactive Flow in Single Phase Hydrothermal Systems, *American Journal of Science*, *294*, 529–592.

Steefel, C., et al. (2015), Reactive transport codes for subsurface environmental simulation, *Computational Geosciences*, *19*(3), 445–478, doi:10.1007/s10596-014-9443-x.

Tompson, A. F. B., and D. Dougherty (1992), Particle-grid methods for reacting flows in porous-media with application to Fisher equation, *Appl. Math. Model.* 16 (7), 374–383.

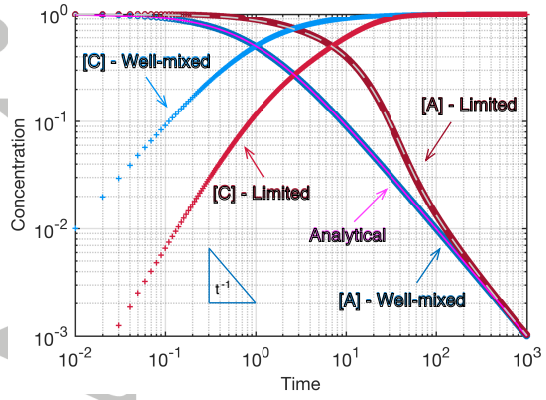

Figure 1. Analytical validation of the CRP algorithm against the analytical solution of Eq 7 along with a mixing-limited case for comparison ("Limited"). The time delay in the reaction rate of the latter is a reflection of the mixing rate and relative overlap of the two reactants. Scaling proportionate to t^{-1} is characteristic of a well-mixed system. The dashed line is a finite difference solution of the mixing-limited diffusion-reaction system.

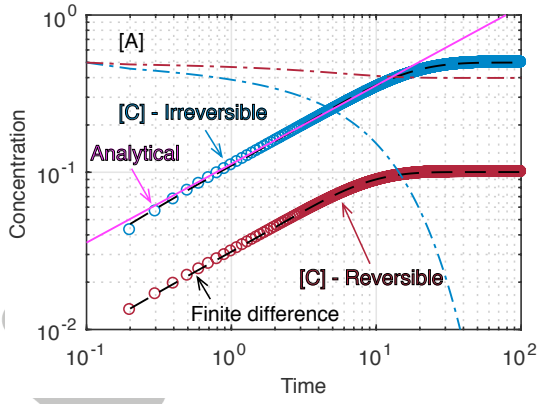

Figure 2. CRP based simulation of the irreversible, equilibrium reaction of *Gramling et al.* [2002] and the analytical solution where the reactant mass is shown by the dashed lines and the product mass is shown as the circles. The late time departure is the result of the finite sized domain used in these simulations. A reversible reaction is also shown for comparison where the reactants are not entirely consumed. The black dashed lines superimposed on the product concentrations are from a finite difference solution of the same systems.

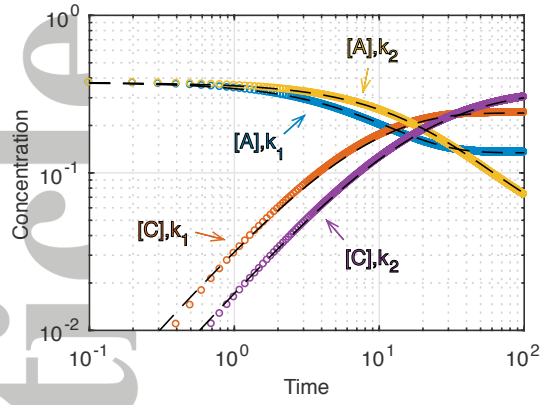

Figure 3. Simulation of reversible kinetic reactions for $k_{1,f} = 2.0\text{x}10^{-1}$, $k_{1,r} = 1.5\text{x}10^{-2}$ and $k_{2,f} = 1.0\text{x}10^{-2}$, $k_{2,r} = 1.0\text{x}10^{-3}$. The well-mixed ODE solutions are the dashed lines overlaid on each component. This simulation uses only 750 particles and this causes a slight overestimation of $[C]$ at intermediate times, but the late time behavior of the model is exact.

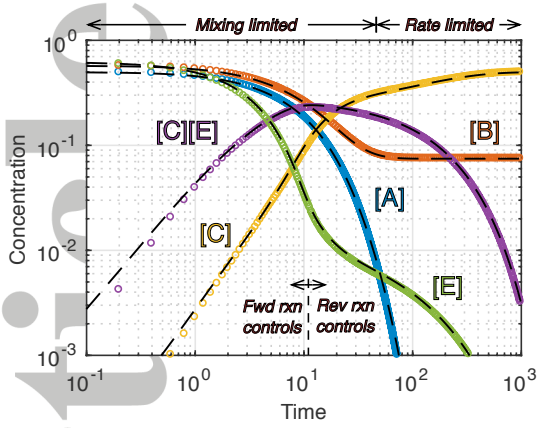

Figure 4. Temporal evolution of concentration in the decay chain simulation. The mixing limited reaction of (8a) is limiting at early time, producing C that reacts with the abundant E to form CE. Later, the breakdown of $[E]$ causes the reverse reaction of (8b) to dominate, which now produces E and slows its decay. This is just one example of the complex interactions that can now be simulated in a Lagrangian setting. The dashed black lines are from a finite-difference solution of the same system.

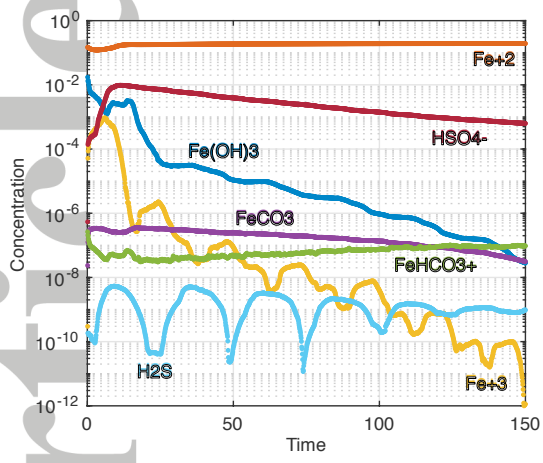

Figure 5. Total concentration of selected aqueous species over time for the acid-mine drainage example. This illustrative example combines all of the components of the Lagrangian CRP framework: mass transfer, advection, dispersion, diffusion and the PhreeqcRM reaction engine. The sequential changes reflect gradual shifts in chemistry as the plume passes the outcrop multiple times.

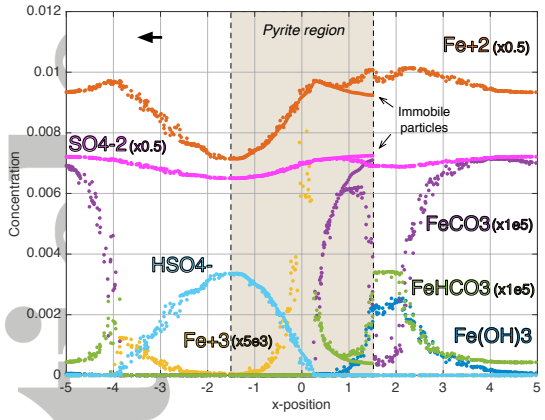

Figure 6. Spatial distribution of selected aqueous species at $t = 15$, some of which have been scaled to highlight their interactions (scale factors are in parentheses). The immobile particles on the upstream edge of the pyrite region are in disequilibrium with the mobile particles, and this is erased as the mobile particles move farther across the outcrop. This figure also clearly shows that multiple chemical interfaces are present, even though only one slug of clean water was added to the system.

Figure 1.

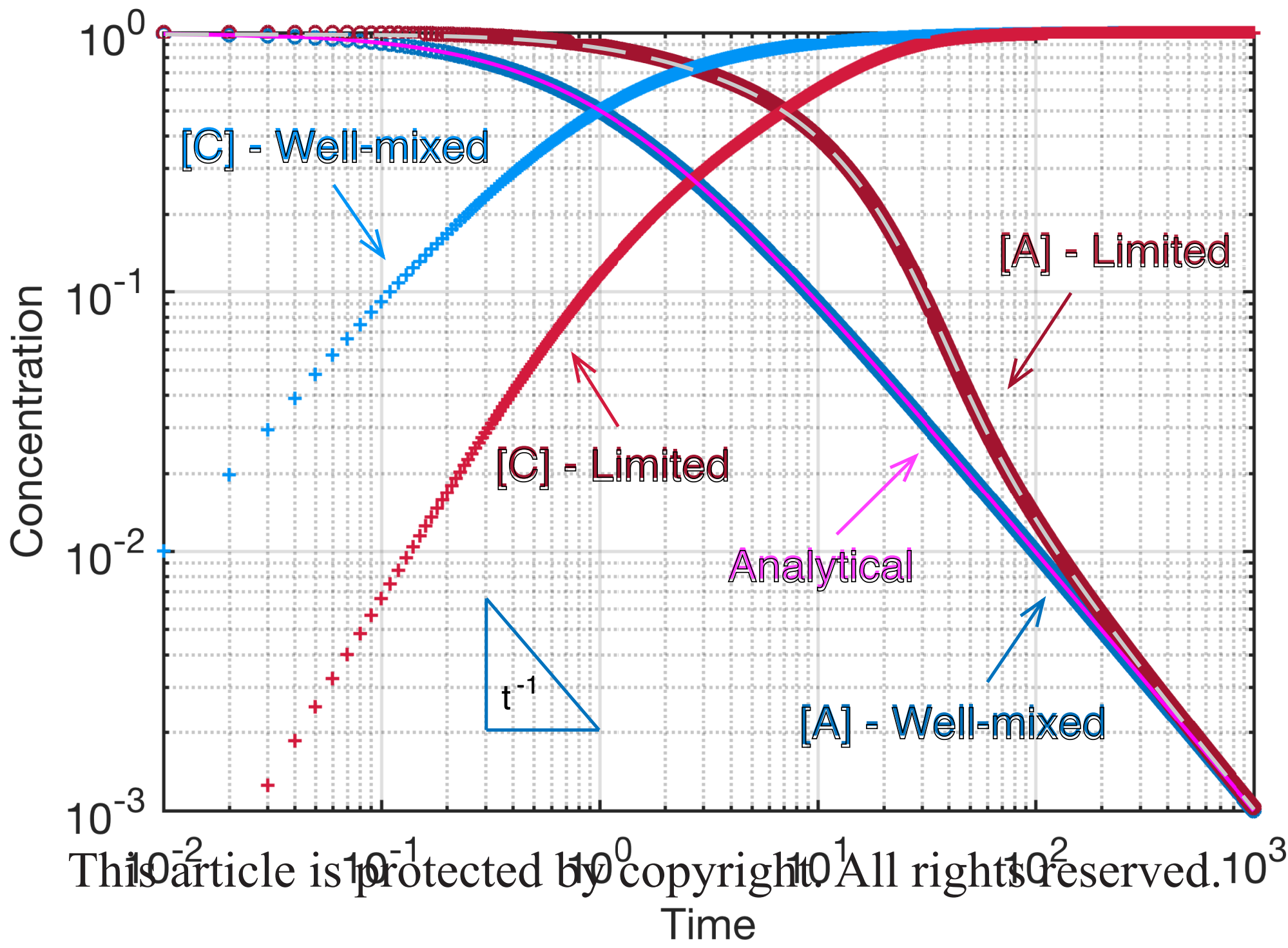

Figure 2.

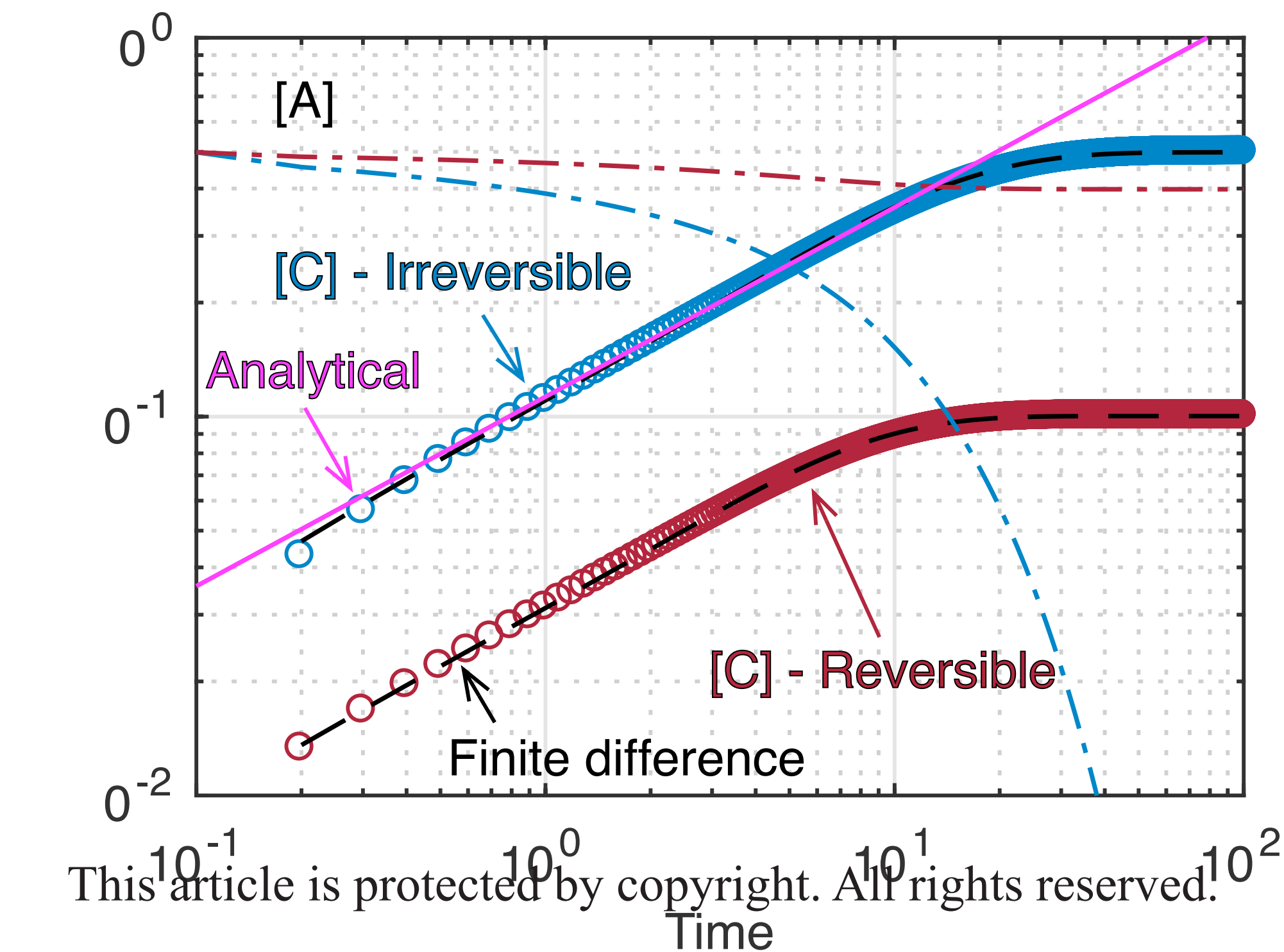

Figure 3.

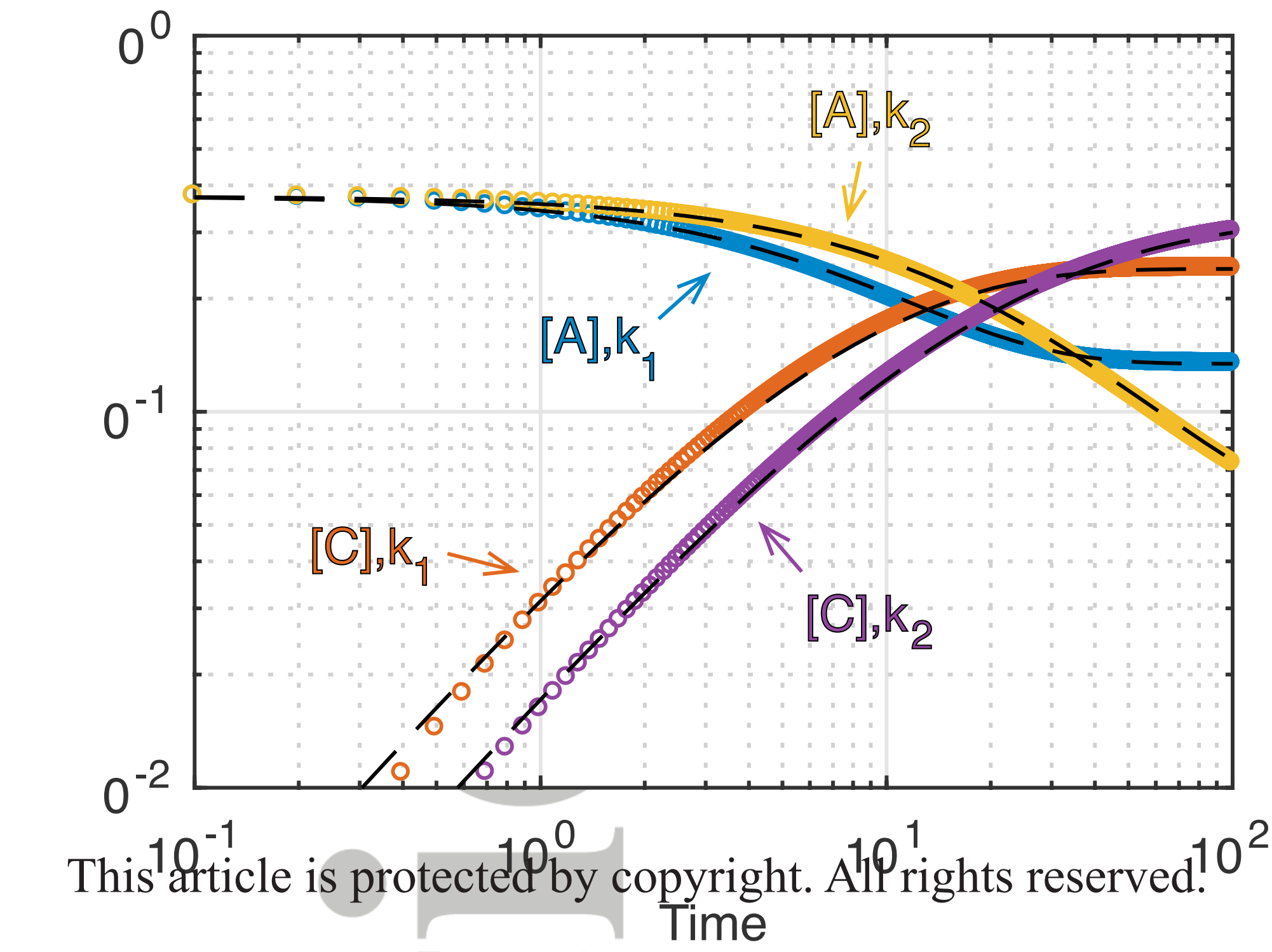

Figure 4.

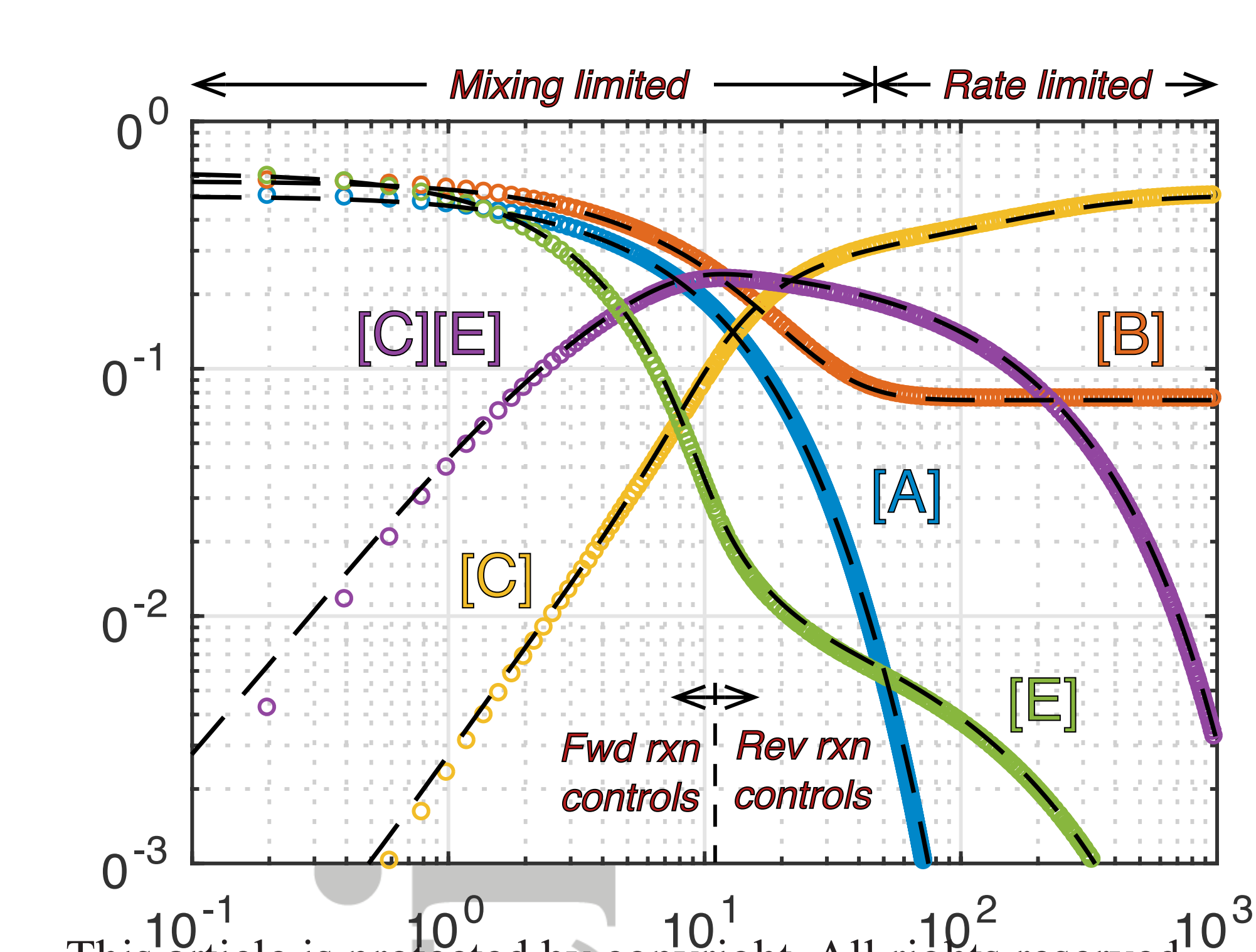

Figure 5.

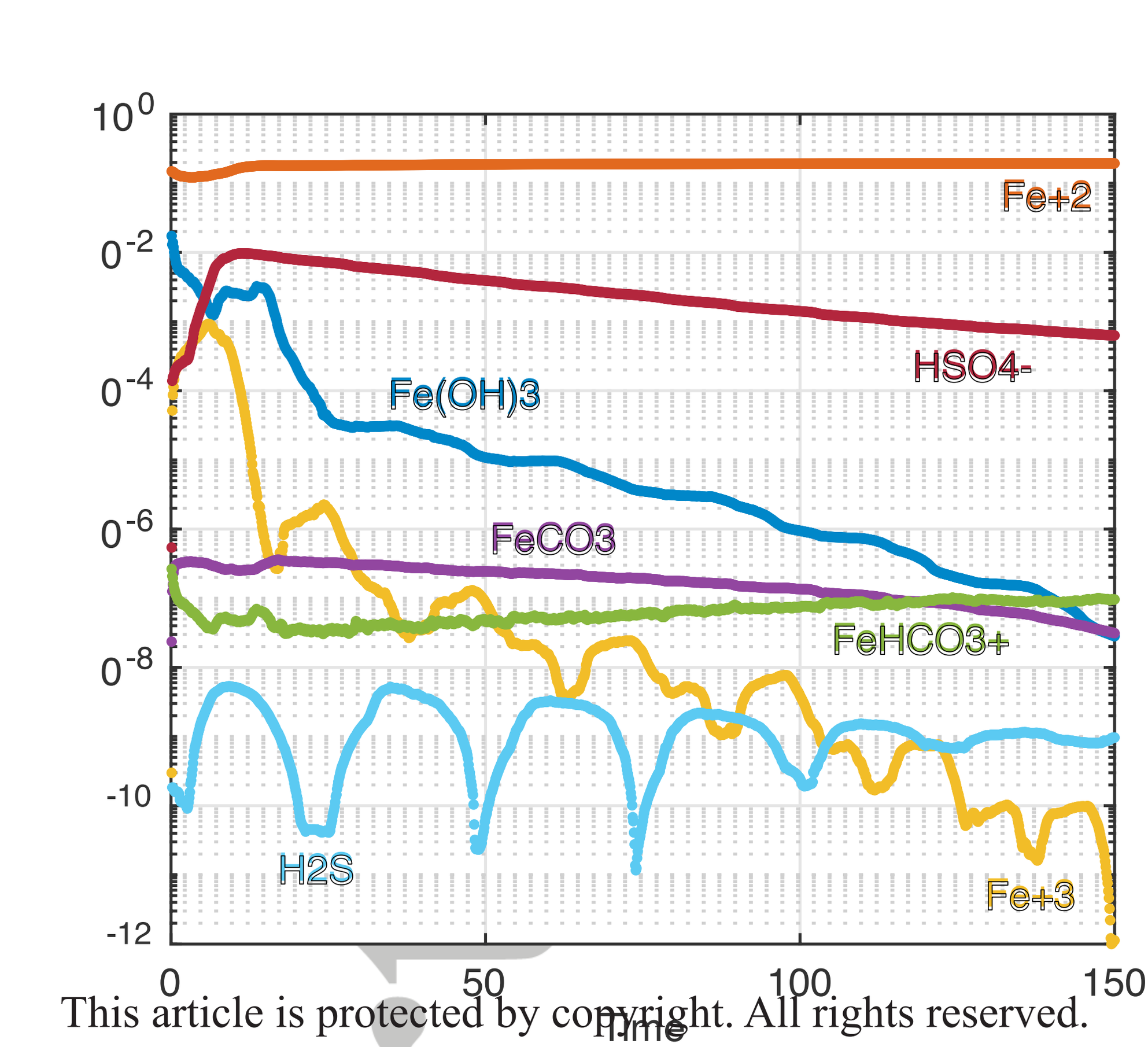

Figure 6.